

Shape Control of Single Crystalline Bismuth Nanostructures

Wen Zhong Wang,* Bed Poudel, Yi Ma, and Z. F. Ren*

Department of Physics, Boston College, Chestnut Hill, Massachusetts 02467

Received: June 5, 2006; In Final Form: October 15, 2006

A synthesis approach for shape control of single crystalline Bi nanostructures has been developed. By controlling the molar ratio of PVP and Bi in a polyol process, Bi nanocubes with an edge length of ~ 60 – 80 nm, triangular nanoplates with an edge length of 200 – 500 nm, and nanospheres with an average diameter of 75 nm have been successfully synthesized. In the same synthetic process, Bi nanobelts with lengths of up to 80 μm and widths of up to 0.6 μm were synthesized in large quantities by introducing a trace amount of Fe^{3+} species into the reaction system. These single crystalline nanostructure Bi materials are expected to find potential applications in a variety of areas including high efficiency thermoelectric devices.

Introduction

Bismuth (Bi), as a semimetal with a rhombohedral structure and a very small band gap, has attracted extensive interest recently as a potential good room temperature thermoelectric material due to its low effective mass, highly anisotropic Fermi surface, and potential to induce a semimetal–semiconductor transition with decreasing crystallite size.¹ Theoretical studies predicted that nanostructured Bi should have a significantly enhanced thermoelectric figure of merit,² which have stimulated great efforts to synthesize Bi nanostructured materials.^{3–5} Most of the previous work has been focused on synthesis of one-dimensional Bi nanowires using rigid inorganic or polymer templates.^{6,7} Recently, there are a few reports on the synthesis of Bi nanoparticles by a variety of methods, such as inverse micelles,⁸ radiolytic reduction in aqueous solution,⁹ high temperature organic solution reduction,¹⁰ and solution-based reduction.^{11,12} However, the morphology of the Bi nanoparticles prepared by these methods are usually spherical. Up to now, there is no report on the control of the shape of Bi nanocrystals.

Generally, the shape of a nanostructure may enable tailoring the electronic, optical, magnetic, and catalytic properties of a functional material. A great deal of effort has therefore been devoted to the synthesis of nanostructures with well-controlled shapes.¹³ Shape-controlled preparation of a number of metal and alloy nanoparticles have been achieved, such as Co, Ag, Au, Pt, Pd, Rh, Ir, and FePt, by reduction of salt compounds or thermal decomposition of organometallic precursors in the presence of surfactants, polymers, biomolecules, and coordinating ligands.¹⁴ Here we demonstrate that the shape and size of nanoscale Bi could be controlled by changing the ratio of the concentration of the capping polymer material to the concentration of the Bi cations in the polyol process^{15–18} or by introducing a trace amount of Fe^{3+} species to the reaction system. Nanocubes, triangular nanoplates, nanospheres, and nanobelts were synthesized using such approach and reported here.

Experimental Section

Bi nanocrystals with controlled shape and size were prepared by a polyol process. The primary reaction involved the reduction of NaBiO_3 (99.6%, Aldrich) with ethylene glycol (EG, 99.8%,

Aldrich) in the presence of the capping polymer poly(vinyl pyrrolidone) (PVP, MW 1 300 000) (Aldrich) or a trace amount of Fe^{3+} (FeCl_3 , 99%, Aldrich) at 200 $^\circ\text{C}$ in a Parr reactor (125 mL, model 4750, Parr Company, Moline, IL). The experiments suggested that the morphologies of the product are strongly dependent on the molar ratio of PVP and Bi, and the trace amount of Fe^{3+} .

Field emission scanning electron microscopy (SEM, JEOL 6340F) and transmission electron microscopy (TEM, JEOL 2010F), high-resolution TEM (HRTEM), selected area electron diffraction (SAED), and X-ray diffraction (XRD) were used to characterize the Bi nanostructures.

Results and Discussions

When the molar ratio of PVP and Bi was kept at 1.6, single crystalline Bi nanocubes were obtained. Figures 1a and 1b show the SEM images of the as-prepared Bi nanocubes with different magnifications. The low-magnification image (Figure 1a) clearly indicates the abundance and narrow size distribution with an edge length of ~ 60 – 80 nm. The high magnification image (Figure 1b) demonstrates the good cubic shape with smooth surfaces. Figure 1c shows the typical 2-theta XRD pattern of the as-prepared Bi nanocubes. All diffraction peaks were indexed to the rhombohedral Bi structure (JCPDS No. 05–0519, $R\bar{3}m$).

Figure 2 shows the TEM and HRTEM images of the Bi nanocubes. The low magnification TEM image (Figure 2a) demonstrates that the Bi nanocrystals have fairly uniform size with cubic structure of an average edge length of ~ 70 nm, consistent with the results of SEM observations as shown in Figure 1a. Figure 2b shows the TEM image of an individual Bi nanocrystal, indicating a cubic shape. Figure 2c shows the TEM image of a single nanocube used for the studies of HRTEM and SAED (inset in Figure 2c) obtained by aligning the electron beam perpendicular to one of the faces of the cube. The square diffraction patterns were indexed based on a rhombohedral cell with a lattice parameter of $a = 4.546$ and $c = 11.860$ \AA , indicating the single-crystal nature. Figure 2d shows the HRTEM image taken from the marked area (area I in Figure 2c). The clear two-dimensional (2D) lattice fringes demonstrate that the cube is highly crystallized. The spacing of 0.32 nm corresponds to the (012) planes of Bi, indicating that one of the cubic faces is (012), stabilized by the PVP:Bi molar ratio

* Corresponding author. E-mail: renzh@bc.edu; wangwm@bc.edu.

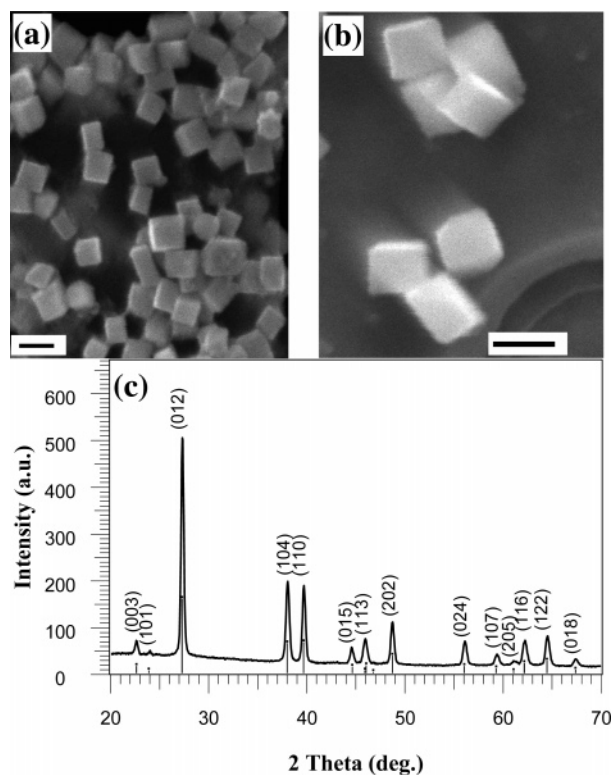


Figure 1. (a) Low- and (b) high-magnification SEM images; the scale bars represent 100 nm. (c) XRD pattern of the as-prepared Bi nanocubes.

of 1.6. Figures 2e and 2f are the HRTEM images taken along the edge (area II in Figure 2c) and around the corner (area III in Figure 2c), respectively. Both 2e and 2f show the Bi crystals are free of oxide layer on the surface, an indication of good stability of the cubes in air.

When the molar ratio of PVP and Bi was reduced to 0.8, single crystalline Bi triangular nanoplates were obtained together with cubic and irregular shaped nanoparticles. The percentage of triangular nanoplates in the sample is about 30%. Figures 3a and 3b show the low- and high-magnification TEM images of the triangular nanoplates, respectively. The TEM images indicate that the lengths of the three edges of each triangular nanoplate are equal in the range of 200–500 nm. Figure 3c shows the TEM image of a single triangular nanoplate with the SAED as the inset obtained by aligning the electron beam perpendicular to the face of this plate. The hexagonal symmetric diffraction pattern indicates the single crystalline nature of the nanoplate. Figure 3d shows the HRTEM image with clear lattice fringes that confirm the highly crystalline nature. The spacing of 0.222 nm corresponds to the (110) planes of Bi. From the SAED pattern (inset, Figure 3c), we know that the crystal plane is (002) that is stabilized by the PVP:Bi molar ratio of 0.8. However, if the molar ratio of PVP and Bi was further reduced to 0 or increased to 5, spherical nanoparticles were formed. Figure 3e shows the TEM image of the product prepared in the absence of PVP. The product is composed of spherical particles with wide diameter distribution ranging from 20 to 200 nm. When the molar ratio is increased to 5, the product is composed of uniform spheres with an average diameter of 75 nm as shown in Figure 3f.

The above experimental results indicate that the molar ratio of PVP and Bi plays a key role for the shape control of Bi nanocrystals. We think that PVP plays multiple roles in our synthetic system. It acts not only as the shape control agent but also as the stabilizing agent. The fact that only spheres with

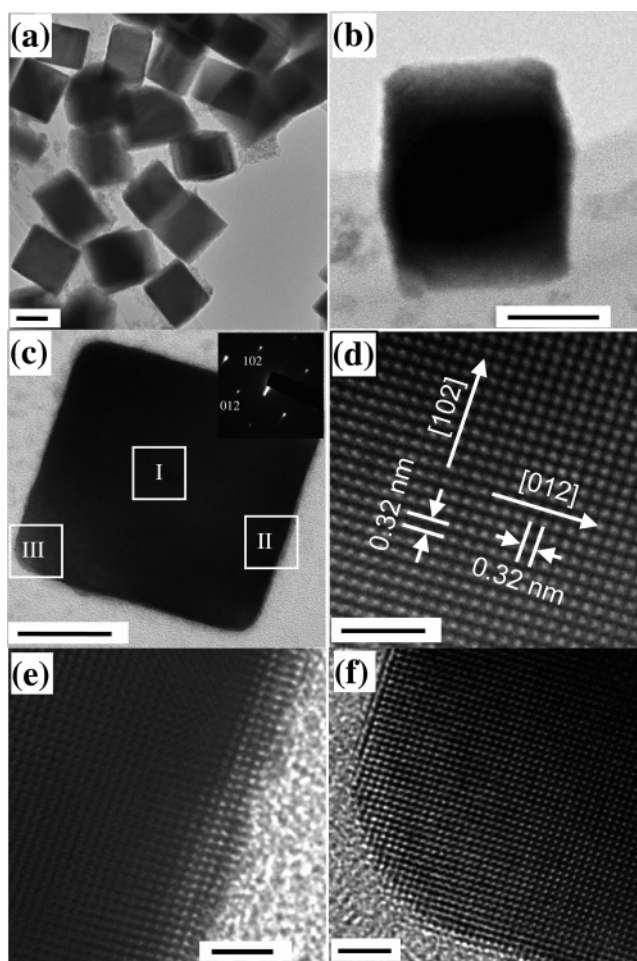


Figure 2. (a) Typical TEM images of the as-prepared Bi nanocubes; the scale bar represents 50 nm. (b) TEM image of an individual Bi nanocrystal showing good cubic shape; the scale bar represents 50 nm. (c) TEM image and the corresponding SAED pattern of a single cube; the scale bar represents 20 nm. (d–f) HRTEM images taken from the marked areas I, II, and III in Figure 2c, respectively, the scale bars represent 2 nm.

wide diameter distribution were obtained in the absence of PVP (Figure 3e) indicates that some Bi tiny crystals aggregate to form big particles due to lack of protection from the stabilizing agent PVP. However, when the molar ratio is increased to 5, excess PVP molecules could act as stabilizing agents to protect particles from aggregating to form big particles. On the other hand, PVP acts as a shape-controlling agent for the formation of Bi nanocubes and triangular nanoplates. It has been reported that the capping organic molecules could modulate the kinetics of the crystal growth and determine the subsequent shape of the crystals.^{13c,19–21} For the present case, PVP molecules could adsorb onto the surfaces of Bi crystals through O–Bi bonding as reported in previous work.⁴ PVP molecules adsorbed on some surfaces of the Bi crystals could significantly decrease their growth rates and lead to highly anisotropic growth. A decrease in PVP concentration leads to an ineffectively selective adsorption of the PVP molecule and its respective counter ions on the Bi crystal faces, resulting in the formation of various morphologies, such as triangular nanoplates and cubic and irregular shape. As for high PVP concentration, excess PVP molecules could decrease the interaction between ethylene glycol and Bi nanocrystals, so the isotropic growth of Bi crystals was subsequently realized resulting in the formation of Bi nanospheres with uniform size. Therefore the selective interaction between PVP and various crystallographic planes of Bi plays

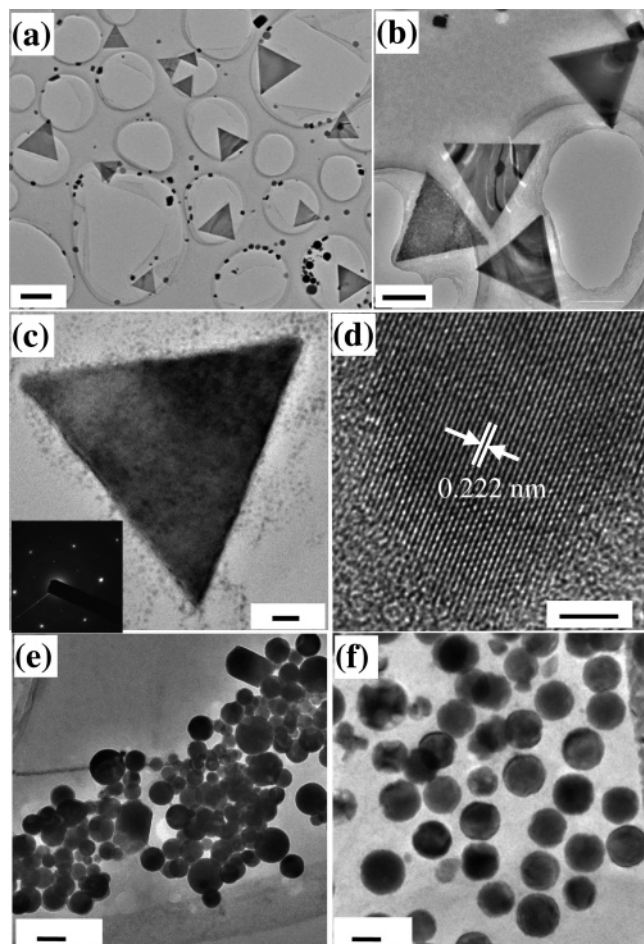


Figure 3. Typical TEM images of the Bi triangular nanoplates at (a) low- and (b) high-magnification; the scale bars represent 500 and 200 nm respectively. (c) TEM image and the corresponding SAED pattern of a single nanoplate; the scale bar represents 20 nm. (d) HRTEM image of the nanoplate of part c; the scale bar represents 2 nm. (e) TEM image of the as-prepared products without PVP; the scale bar represent 100 nm. (f) TEM images of the as-prepared products with the molar ratio of PVP and Bi of 5; the scale bar represents 50 nm.

the major role for the formation of Bi nanocubes and triangular nanoplates, although the exact bonding geometry and the nature of the selective adsorption of PVP on various crystallographic planes of Bi are still not clear. The fundamental basis of shape selectivity for this system has yet to be fully understood.

It was also found that introduction of a trace amount of Fe^{3+} species to the reaction system greatly changed the shape of the final Bi nanocrystals. Figure 4 shows the SEM images of the Bi nanobelts prepared in the presence of Fe^{3+} species with the molar ratio of PVP and Bi of 1.6. The low magnification image (Figure 4a) indicates that large quantities of nanobelts are formed with lengths up to 80 μm . The high magnification image (Figure 4b) demonstrates that the width of the nanobelts is up to 0.6 μm . Figure 4c shows the typical XRD pattern of the as-prepared Bi nanobelts. All the diffraction peaks were indexed to the rhombohedral Bi structure (JCPDS No. 05-0519, $R\bar{3}m$).

Figure 5 shows the typical TEM images of the Bi nanobelts with different magnifications. The low magnification image (Figure 5a) indicates that the nanobelts display a broad width distribution from 50 to 600 nm. High magnification image (Figure 5b) indicates that the nanobelts are transparent under the irradiation of electric beam, revealing that the thickness of the nanobelts is very thin although the width is up to 0.6 μm . Figure 5c shows the TEM image of a single nanobelt used for

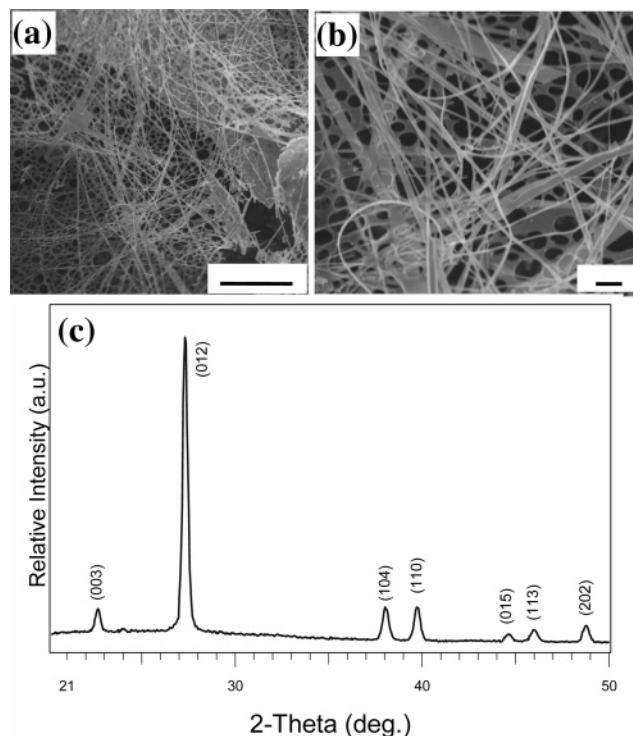


Figure 4. SEM images of the as- prepared Bi nanobelts at (a) low- and (b) high-magnification; the scale bars represent 10 and 1 μm , respectively. (c) XRD pattern of the Bi nanobelts.

the studies of HRTEM and SAED obtained by aligning the electron beam perpendicular to the face of the belt. The square diffraction pattern was indexed on the basis of a rhombohedral cell with a lattice parameter of $a = 4.546$ and $c = 11.860$ \AA , indicating that the Bi nanobelt is a single crystal. Figure 5d shows the HRTEM image of the nanobelt shown in Figure 5c. The clear 2D lattice fringes demonstrate that the belt is highly crystallized. The spacing of 0.32 nm corresponds to the (012) planes of Bi, from which we determined that the crystal plane is (221), stabilized by PVP:Bi ratio of 1.6 and a trace amount of Fe^{3+} . From TEM image (Figure 5c) and the corresponding SAED pattern (inset in Figure 5c), the growth direction of the Bi nanobelt is derived as $[1\bar{1}0]$.

It is worthwhile to elucidate the growth mechanism of the nanobelts. As reported in previous works, the organic molecules could play the roles of a surface modifier and assembling agents during the formation of nanostructures by oriented attachment mechanism, because the organic molecules adsorbed on a crystallographically specific surface can modify oriented attachment mechanism by changing the surface energy and also preventing contact between the surfaces on which adsorption has selectively occurred.²²⁻²⁴ Thus, in our current case, the freshly formed Bi nanocrystals could align and subsequently form nanobelts in the presence of assembling agent PVP. The conclusions could be verified by extensive and careful TEM and HRTEM observations. In TEM examinations, we found that some belts were composed of fused nanoparticles (Figure 5e), and further HRTEM studies indicated that these fused nanoparticles had the same growth direction (Figure 5f), revealing that aligning of orientations might have happened before they connected to each other. Therefore the Bi nanobelts were probably formed through the oriented attachment mechanism found in the growth of other low-dimensional nanostructures.^{22,25-27} On the basis of the above experimental results and analysis, we speculate that the formation process of Bi nanobelts could be as the following: (i) when a small amount of Fe^{3+} was added

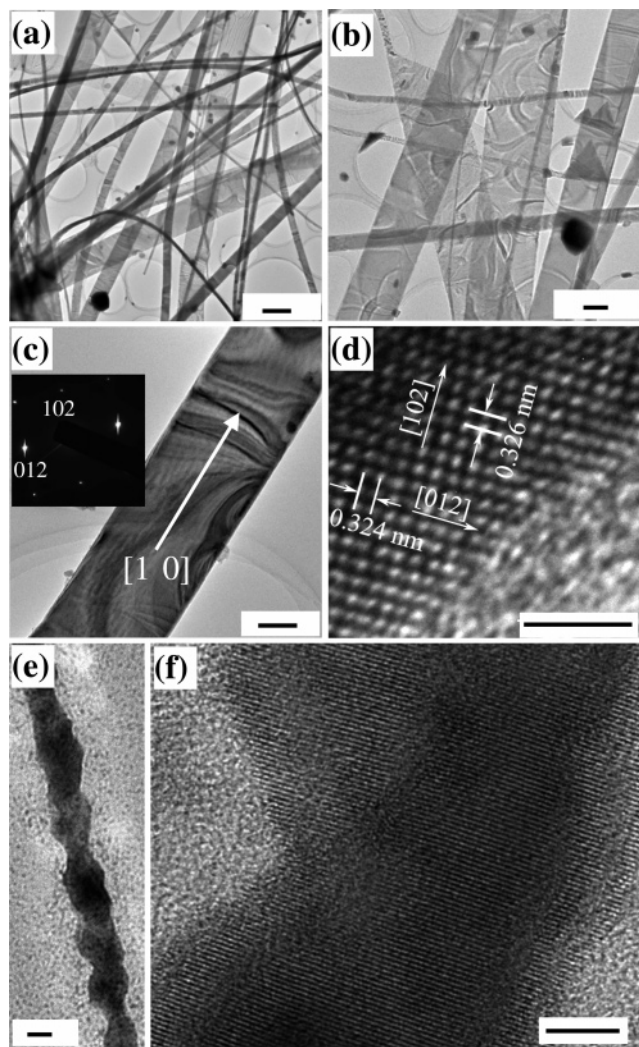


Figure 5. Typical TEM images of the Bi nanobelts at (a) low- and (b) high-magnification; the scale bars represent 500 and 200 nm, respectively. (c) TEM image and the corresponding SAED pattern of a single nanobelt; the scale bar represents 100 nm. (d) HRTEM image of the nanobelt shown in part c; the scale bar represents 2 nm. (e) A typical TEM image of an individual belt, clearly indicating that the belt is composed of fused nanoparticles, the scale bar represents 20 nm. (f) HRTEM image of part e indicating that the fused nanoparticles have the same growth direction; the scale bar represents 5 nm.

into the system, the reduction of Bi^{3+} was significantly slowed down, resulting in a substantial decrease of the nucleation rate of the Bi nanoparticles; (ii) the nanoparticles aligned to the same direction and then connected to each other to form wire-like structures induced by assembling agent PVP; (iii) with the prolongation of reaction time and the improvement of crystallinity, these nanoparticles further fused and then grew into single-crystal Bi nanobelts. The role of Fe^{3+} is to oxidize $\text{Bi}(0)$ to Bi(III) and thus greatly reduce the nucleation density of Bi. We think that the role of Fe^{3+} in our case is the same as that in the cases of platinum nanowires¹⁷ or palladium nanostructures.¹⁸ The detailed study on the growth mechanism of Bi nanobelt is still under way. Our experimental results indicate that the Bi nanostructures with different morphology can be synthesized by controlling the molar ration of PVP and Bi, or introducing a trace amount of Fe^{3+} species in the polyol process. The relationship between synthesis conditions and the structures of the crystals is summarized in Table 1.

TABLE 1: The Relationship Between the Synthesis Conditions and the Structures of the Crystals

molar ratio of PVP/Bi	morphology	stabilized planes
0	sphere	
0.8	triangular nanoplate (30%) with cubic and irregular shape	(002)
1.6	nanocube	(012), (102), and (221)
5	nanosphere	
1.6 with the presence of a trace amount of Fe^{3+}	nanobelt	(221)

Conclusions

In summary, Bi nanoscale materials with different shapes have been successfully synthesized by a polymer-assisted polyol process. The molar ratio of PVP and Bi played an important role for the formation of Bi nanocubes, triangular nanoplates, and spheres. The experiments also indicated that introduction of a trace amount of Fe^{3+} species greatly reduced the nucleation density of Bi and the growth rate, leading to the formation of single-crystal Bi nanobelts.

Acknowledgment. The work is funded by NSF NIRT 0506830.

References and Notes

- (1) (a) Hicks, L. D.; Dresselhaus, M. S. *Phys. Rev. B* **1993**, *47*, 12727. (b) Koga, T.; Harman, T. C.; Cronin, S. B.; Dresselhaus, M. S. *Phys. Rev. B* **1999**, *60*, 14286.
- (2) Hicks, L. D.; Dresselhaus, M. S. *Phys. Rev. B* **1993**, *47*, 16631. (b) Sun, X.; Zhang, Z.; Dresselhaus, M. S. *Appl. Phys. Lett.* **1999**, *74*, 4005. (c) Lin, Y.-M.; Sun, X.; Dresselhaus, M. S. *Phys. Rev. B* **2000**, *62*, 4610.
- (3) Yu, H.; Gibbons, P. C.; Buhro, W. E. *J. Mater. Chem.* **2004**, *14*, 595.
- (4) Wang, J.; Wang, X.; Peng, Q.; Li, Y. D. *Inorg. Chem.* **2004**, *43*, 7552.
- (5) Fu, R. L.; Xu, S.; Lu, Y. N.; Zhu, J. J. *Cryst. Growth Des.* **2005**, *5*, 1379.
- (6) Dresselhaus, M. S.; Zhang, Z.; Sun, X.; Ying, J. Y.; Heremans, J.; Dresselhaus, G.; Chen, G. *Mater. Res. Soc. Symp. Proc.* **1999**, *545*, 215.
- (7) Heremans, J. P.; Thrush, C. M.; Morelli, D. T.; Wu, M. C. *Phys. Rev. Lett.* **2002**, *88*, 216801.
- (8) Foos, E. E.; Stroud, R. M.; Berry, A. D.; Snow, A. W.; Armistead, J. P. *J. Am. Chem. Soc.* **2000**, *122*, 7114.
- (9) Gutierrez, M.; Henglein, A. *J. Phys. Chem.* **1996**, *100*, 7656.
- (10) Fang, J. Y.; Stokes, K. L.; Zhou, W. L.; Wang, W. D.; Lin, J. *Chem. Commun.* **2001**, 18, 1872.
- (11) Balan, L.; Schneider, R.; Billaud, D.; Fort, Y.; Ghanbaja, J. *Nanotechnology* **2004**, *15*, 940.
- (12) Wang, Y. W.; Hong, B. H.; Kim, K. S. *J. Phys. Chem. B* **2005**, *109*, 7067.
- (13) (a) Wang, Z. L.; Ahmad, T. S.; El-Sayed, M. A. *Surf. Sci.* **1997**, *380*, 302. (b) Wang, Z. L. *J. Phys. Chem. B* **2000**, *104*, 1153. (c) Milliron, D. J.; Hughes, S. M.; Cui, Y.; Manna, L.; Li, J.; Wang, L. W.; Alivisatos, A. P. *Nature* **2004**, *430*, 190. (d) Peng, X.; Manna, L.; Yang, W.; Wickham, J.; Scher, E.; Kadavanich, A.; Alivisatos, A. P. *Nature* **2000**, *404*, 59. (e) Kim, F.; Connor, S.; Sond, H.; Kuykendall, T.; Yang, P. *Angew. Chem., Int. Ed.* **2004**, *43*, 3673. (f) Tapan, T. K.; Murphy, C. J. *J. Am. Chem. Soc.* **2004**, *126*, 8648. (g) Chen, S.; Wang, Z.; Ballato, J.; Foulger, S. H.; Carroll, D. L. *J. Am. Chem. Soc.* **2003**, *125*, 16186. (h) Pileni, M. *Nat. Mater.* **2003**, *2*, 145.
- (14) (a) Sun, S.; Murray, C. B.; Weller, D.; Folks, L.; Moser, A. *Science* **2000**, *287*, 1989. (b) Chen, S.; Wang, Z. L.; Ballato, J.; Foulger, S. H.; Carroll, D. L. *J. Am. Chem. Soc.* **2003**, *125*, 16186. (c) Caswell, K. K.; Wilson, J. N.; Bunz, U. H. F.; Murphy, C. J. *J. Am. Chem. Soc.* **2003**, *125*, 13914. (d) Kim, F.; Connor, S.; Song, H.; Kuykendall, T.; Yang, P. *Angew. Chem., Int. Ed.* **2004**, *43*, 3673. (e) Narayanan, R.; El-Sayed, M. A. *J. Phys. Chem. B* **2004**, *108*, 5726. (f) Hao, E.; Bailey, R. C.; Schatz, G. C.; Hupp, J. T.; Li, S. *Nano Lett.* **2004**, *4*, 327. (g) Yin, Y.; Rioux, R. M.; Erdonmez, C. K.; Hughes, S.; Somorjai, G. A.; Alivisatos, A. P. *Science* **2004**, *304*, 711.
- (15) Fievet, F.; Lagier, J. P.; Figlarz, M. *MRS Bulletin* **1989**, December, 29.
- (16) Wang, Y. L.; Xia, Y. N. *Nano Lett* **2004**, *4*, 2047.

- (17) Cheng, J.; Herricks, T.; Geissler, M.; Xia, Y. N. *J. Am. Chem. Soc.* **2004**, *126*, 10854.
- (18) Xiong, Y.; McLellan, J. M.; Chen, J.; Yin, Y.; Li, Z. Y.; Xia, Y. N. *J. Am. Chem. Soc.* **2005**, *127*, 17118.
- (19) (a) Sun, Y.; Xia, Y. *Adv. Mater.* **2002**, *14*, 833. (b) Sun, Y.; Yin, Y.; Mayers, B. T.; Herricks, T.; Xia, Y. *Chem. Mater.* **2002**, *14*, 4736.
- (20) Peng, X. *Adv. Mater.* **2003**, *15*, 459.
- (21) Lee, S. M.; Cho, S. N.; Cheon, J. *Adv. Mater.* **2003**, *15*, 441.
- (22) Penn, R. L.; Banfield, J. F. *Geochim. Cosmochim. Acta* **1999**, *63*, 1549.
- (23) Polleux J.; Pinna, N.; Antonietti, M.; Niederberger, M. *Adv. Mater.* **2004**, *16*, 436.
- (24) J.; Pinna, N.; Pinna, N.; Antonietti, M.; Hess, C.; Wild, U.; Schlögl, R.; Niederberger, M. *Chem. Eur. J.* **2005**, *11*, 3541.
- (25) Oskam, G.; Nellore, A.; Penn, R. L.; Searson, P. C. *J. Phys. Chem. B* **2003**, *107*, 1734.
- (26) Oskam, G.; Hu, Z.; Penn, R. L.; Pesika, N.; Searson, P. C. *Phys. Rev. E* **2002**, *66*, 11403.
- (27) Alivisatos, A. P. *Science* **2000**, *289*, 736.